

SMALL STRAIN SHEAR MODULUS OF CLAY SEDIMENTATION  
IN A STATE OF NORMAL CONSOLIDATIONSATORU SHIBUYA<sup>i)</sup> and TOSHIYUKI MITACHI<sup>ii)</sup>

## ABSTRACT

In this paper, consideration is given as to how to characterize depth-variation for the small-strain shear modulus of natural clay sedimentation, in a state of normal consolidation. A case study was carried out for a relatively uniform clay layer deposited in the Holocene era. Initially, the effects of both strain and in-situ stress levels on secant shear modulus were carefully examined in cyclic torsion shear tests using undisturbed samples, which were recovered at different depths in a test borehole. The range of shear strain examined was between 0.001% and 1%. Similar examination was made for a silty clay using reconstituted samples that were isotropically consolidated at different stress levels. On the basis of the results of these laboratory tests, together with the shear modulus from an in-situ seismic survey, the small-strain shear modulus was formulated in terms of the stress and strain levels, and linked also to undrained shear strength. Interactions of the small strain stiffness between in-situ and laboratory are discussed in depth with an attention paid to the existing aging effect in the original subsurface condition.

**Key words:** aging effect, clay, in-situ seismic survey, laboratory tests, shear modulus, small strain, undrained shear strength (IGC: D6/D7/D5/E8)

## INTRODUCTION

Soil stiffness associated with strains less than 0.1% is designated 'small-strains' in this paper. In an attempt to predict or back-analyze deformation of soils subjected to monotonic and cyclic loading, the small strain stiffness is of major concern to practicing engineers. Burland (1989) pointed out that for monotonic loading problems such as embankment, excavation and foundation footing, the strains induced under working conditions are mostly less than 0.1%. It has also been demonstrated that the boundary values are greatly influenced by the features of small strain stiffness as highlighted by its dependency on the stress and strain levels (Jardine et al., 1986). It is also well-known in soil dynamics that the small strain stiffness governs, to a large extent, the dynamic response of subsoils subjected to cyclic loadings.

Aspects of small strain stiffness have been much better understood in the last decade as a result of recent developments in laboratory instrumentation for measuring soil stiffness over a wide range of shear strain, between 0.0001% and 10% (e.g., Burland and Symes, 1982; Goto et al., 1991). The characteristics observed mostly for reconstituted soil samples are: a) decrease in stiffness initiated at extremely small shear-strain,  $\gamma$ , about 0.002%, b) 'pseudo-elastic' shear modulus,  $G_{\max}$ , confirmed for  $\gamma$

less than about 0.002%, for which the stiffness is the maximum value under a given condition of stress history, and c) beyond this strain level, irrecoverable (or plastic) strains develop when the direction of shear strain increment is reversed (e.g., Tatsuoka and Shibuya, 1992; Shibuya et al., 1992). The term 'pseudo-elastic' is employed based on the fact that  $G_{\max}$  was, under limited conditions, independent of the rate of shear strain, cyclic pre-straining and the type of loading (i.e., monotonic or cyclic loading), however a limiting value of hysteretic damping was involved (see also Shibuya et al., 1995). These observations indicate that depth-variation of  $G_{\max}$  for a natural clay deposit can be estimated from the measurement of in-situ shear wave velocity, which involves little disturbance to the original subsoil.

The  $G_{\max}$  value can be the reference stiffness to characterize the strain-level dependent property of the shear modulus which is observed in the event of both monotonic and cyclic shear. Most hyperbolic stress-strain models, for example, incorporate it, together with the shear strength (e.g., Kondner, 1963; Duncan and Chang, 1970; Hardin and Drnevich, 1972; Tatsuoka and Shibuya, 1992). Despite the fact that, an elasto-plastic model such as Cam clay model is basically more powerful than the fitting-type models, some difficulty occurs in accommodating not only the small strain non-linearity of stiffness but

<sup>i)</sup> Associate Professor, Department of Civil Engineering, Faculty of Engineering, Hokkaido University, Sapporo 060.

<sup>ii)</sup> Professor, ditto.

Manuscript was received for review on February 14, 1994.

Written discussions on this paper should be submitted before July 1, 1995 to the Japanese Society of Soil Mechanics and Foundation Engineering, Sugayama Bldg. 4 F, Kanda Awaji-cho 2-23, Chiyoda-ku, Tokyo 101, Japan. Upon request the closing date may be extended one month.

also the kinematic nature of yield surface(s) into the postulated elastic region (e.g., Jardine, 1992; Atkinson, 1993).

When analyzing ground (subsoil) deformation (or motion) numerically based on such a non-linear soil model, stress-level dependency as well as the strain-level dependency of the small strain stiffness should be properly evaluated in an organized manner. For this purpose, the results of laboratory element tests using 'undisturbed' samples are used exclusively. The stiffness measurements nevertheless involve uncertainties such as effects of sample disturbance, stress release, etc. This is because soil stiffness that can be measured by some in-situ tests (e.g., pressuremeter test) is based on intermediate strains ranging between 0.1 and 1%.

In this paper, depth-variation of the small strain stiffness was carefully examined in cyclic torsion shear tests using undisturbed samples, which were retrieved from a test borehole driven in a uniformly deposited clay layer. Similar examination was made for a reconstituted silty clay using samples that were consolidated at different stress levels. On the basis of these results, the small strain shear modulus is formulated by taking into account the dependency on the stress and strain levels, and also is linked to undrained shear strength. An attempt is also made to generalize the experimental results in order to account for depth-variation of the secant shear modulus for natural clay sedimentation in a normally consolidated state. In the course of discussions, care consideration was given to the "aging effect" which seems to be a key factor linking the shear modulus based on laboratory tests to that from in-situ shear wave velocity. Effects of

stress relief, disturbances during sampling and the anisotropic consolidation, on stiffness are not examined in depth.

## CLAY SAMPLES

Behaviour of two clays, intact samples from the Hachirougata test site and reconstituted samples of Kiyohoro silty clay, was evaluated in the present study.

Hachirougata is located in Akita Prefecture, in the northern part of Honshu, the mainland of the Japanese archipelago. The area used to be a shallow bay which was reclaimed in the 1960's. At this site, a soft clay layer was deposited by sedimentation in a post-glacial age (i.e., Holocene era), and spread over a wide area. This soft clay layer underlies the top sand layer with 2.4 meter thick fill used for the reclamation, up to a 40 meters below the ground surface. The water table was about 1 meter below the ground surface. Available records indicate that the reclaimed fill and subsoils have never been subjected to mechanical overconsolidation.

A test borehole was driven approximately at the middle of the site. Figure 1 shows the profiles of void ratio,  $e$ , yield stress,  $\sigma'_y$ , from load-controlled oedometer tests, undrained shear strengths from unconfined compression test, vane shear test and direct shear box test, and  $G_f$  ( $=\rho_t V_s^2$ ,  $\rho_t$ : total density of soil,  $V_s$ : in-situ shear wave velocity) from seismic cone test. The details of the down-hole seismic cone test and the strength tests have been described by Tanaka et al. (1994) and Tang et al. (1993). As can be seen in Fig. 1, the  $\sigma'_y$  values are close to the current effective overburden pressure,  $\sigma'_v$ , for the entire depth in-

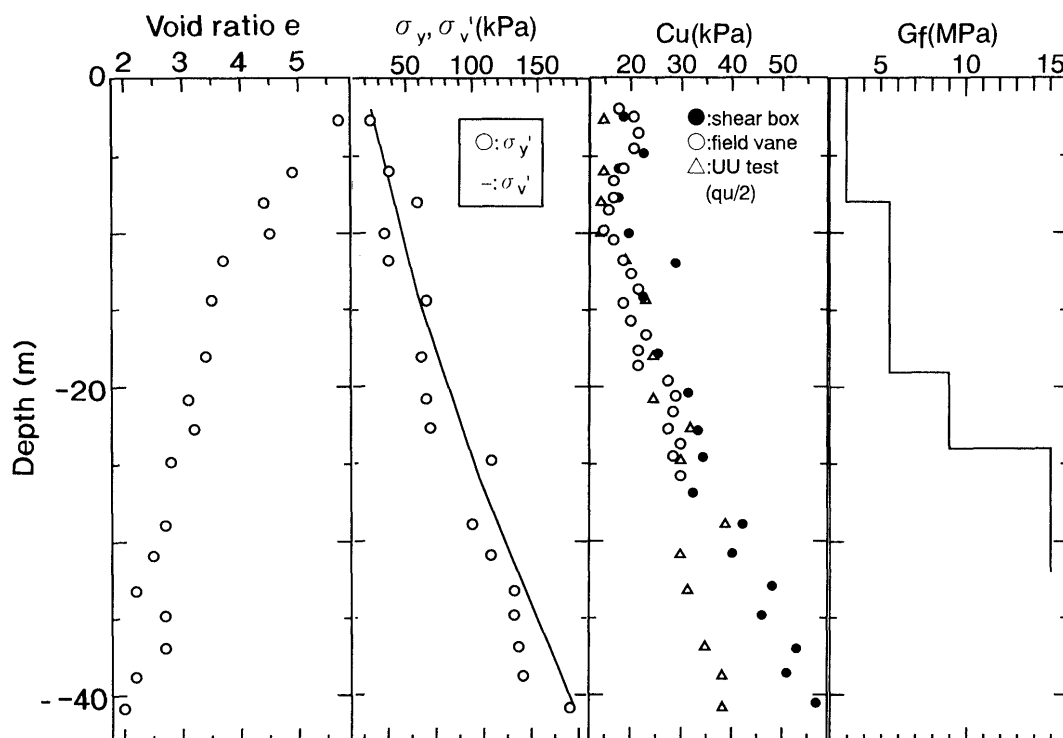


Fig. 1. Results of laboratory and seismic cone tests from a test borehole at Hachirougata site

vestigated. It suggests that the primary consolidation due to reclamation has been completed.

Clay samples were carefully obtained by using two types of samplers; i.e., a thin-wall piston sampler (T-sampler) and an NGI-type sampler (N-sampler), which had inner diameters of 75 mm and 101 mm, respectively. As shown in Table 1, the source of sampler is identified for each sample by labelling the capital T or N in the sample name. It should be mentioned, that the relationship between liquid limit,  $w_L$ , and plasticity index,  $I_p$ , of the clay samples is distributed along Casagrande's A-line.

Kiyohoro silty clay showed Atterberg limits of  $w_L=56\%$  and  $w_p=29\%$ . The mean and maximum particle sizes were 0.03 mm and 0.4 mm, respectively. The material was thoroughly mixed in a batch to a slurry having an initial water content being about twice  $w_L$ . A block of the preconsolidated clay was prepared by consolidating the slurry one-dimensionally at a vertical consolidation pressure of 100 kPa.

### TORSION SHEAR TESTS PERFORMED

Figure 2 shows the configuration of torsion shear apparatus used for tests on the Kiyohoro silty clay. The details of the testing have been given by Shibuya et al. (1995). In the cell, a hollow cylindrical specimen, having a nominal inner radius  $r_i=1.5$  cm, outer radius  $r_o=3.5$

Table 1. Intact samples from Hachirougata site

Test	Depth (m)	$\sigma'_{v, \text{in-situ}}$ (kPa)	$\sigma'_c$ (kPa)	$\rho_s$ (g/cm <sup>3</sup> )	$w_n$ (%)	$w_L$ (%)	$I_p$	$\rho_t$ (g/cm <sup>3</sup> )	$f$ (Hz)	$G_{\text{max}}$ (MPa)
T1	5.1	33	23	2.46	249.7	239	150	1.22	0.05	2.4
T2	6.0	37	25	2.50	214.0	226	152	1.24	0.5	2.1
N29	8.8	44	44	2.58	167.3	166	103	1.29	0.5	2.9
N33	12.8	56	37	2.63	164.0	165	107	1.30	0.5	3.3
T10	15.9	68	45	2.67	130.5	140	89	1.35	0.5	4.5
T11	18.4	77	77	2.66	127.9	137	85	1.37	0.5	11.6
T15	25.0	103	69	2.67	112.6	112	61	1.41	0.05	7.9
T19	30.9	131	131	2.67	90.3	116	75	1.67	0.5	16.7
T24	39.4	173	115	2.61	7.3	122	78	1.54	0.5	16.1

N.B.:  $w_n$ : initial water content of sample,  $\rho_s$ : density of soil particles,  $\rho_t$ : total density

cm and a height of  $H=12$  cm, was isotropically consolidated at a back pressure of 200 kPa to a prescribed value of effective consolidation pressure,  $\sigma'_c$ . It was subjected to shearing using shear-strain control. The torsional shear deformation,  $\theta$ , was imposed by a stepping motor ('B'), and it was measured at the top cap using a proximity transducer (#12) and a potentiometer ('D') for  $\gamma$  less than and larger than 1%, respectively (Teachavorasinskun et al., 1991). Since the stepping motor has no backlash, this torque application system is capable of sharply reversing the direction of the shear strain increment with

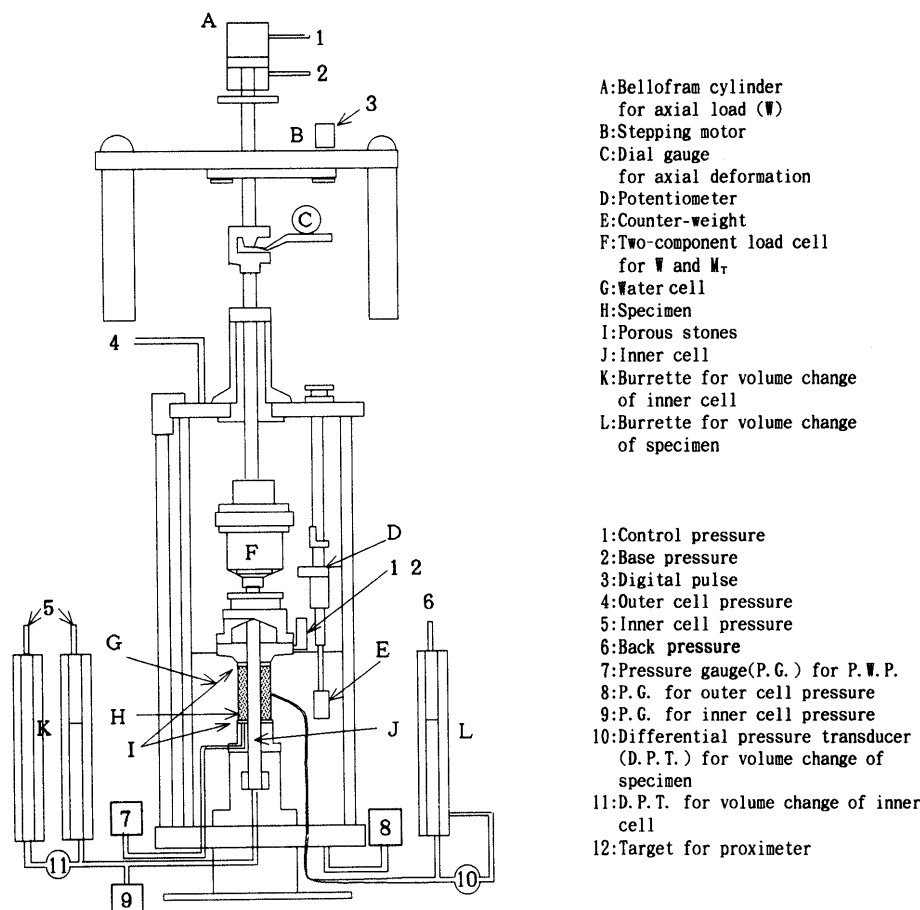


Fig. 2. Torsion shear apparatus used for tests on reconstituted Kiyohoro silty clay

little time-lag (Fig. 3(a)). The axial load and the torque,  $M_T$ , are measured by a load cell ('F') which is installed inside the cell. Note that the measurements of both  $M_T$  and  $\theta$  are virtually free from system compliance.

The average shear stress and strain,  $\tau$  and  $\gamma$ , were esti-

mated using the following equations, respectively (Hight et al., 1983):

$$\tau = 3M_T / \{2\pi(r_o^3 - r_i^3)\} \quad (1)$$

$$\gamma = 2\theta(r_o^3 - r_i^3) / \{3H(r_o^2 - r_i^2)\}. \quad (2)$$

The tests performed are shown in Tables 1 and 2 for the Hachirougata and Kiyohoro clay, respectively. A total of nine cyclic loading (CL) tests were performed on undisturbed samples of Hachirougata clay. Each sample was isotropically consolidated to  $\sigma'_c$  equal to in-situ  $\sigma'_v$  for tests N29, T11 and T19, and to two-third of  $\sigma'_v$  for the rest. The latter refers to a condition that  $\sigma'_c$  was equal to in-situ effective mean stress,  $(1 + 2K_0)\sigma'_v/3$ , assuming a constant value of  $K_0$  equal to 0.5 (n.b.,  $K_0$ : the ratio of horizontal normal stress to  $\sigma'_v$ ). For Kiyohoro silty clay, results of three CL tests and a monotonic loading (ML) test are presented. Note that the  $\sigma'_c$  values were twice or more the preconsolidation pressure of 100 kPa.

The CL tests, except for test T2 on Hachirougata clay, were performed using a popular procedure called multi-stage cyclic shearing. For each stage, a single specimen was subjected to undrained CL with a fixed single amplitude cyclic shear strain,  $\gamma_{SA}$ . A standard number of cycles,  $N$ , was 20 and 11 respectively for Kiyohoro and Hachirougata, respectively. Before the next stage, excess pore pressure which accumulated during CL was fully dissipated. The level of  $\gamma_{SA}$  was raised in stages, starting from about 0.001%. The CL was terminated when  $\gamma_{SA}$  reached its maximum set based on the capacity of the apparatus used. The frequency of loading,  $f$ , was 0.5 and 0.05 Hz for Hachirougata samples, and fixed at 0.01 Hz for tests on Kiyohoro silty clay.

After the sequence of CL was completed, the specimens of Kiyohoro silty clay were subjected to monotonic shear using a constant shear strain rate of 0.00083% ( $8.3 \times 10^{-6}$ ) per second. Note that the rate of shear strain in the CL tests is given by  $4\gamma_{SA}f$ . Accordingly, it increases as  $\gamma_{SA}$  increases at a constant frequency of loading. It has been demonstrated that the rate of shear strain exerted little influence on the observed secant shear modulus for the range of shear-strain rate examined (Shibuya et al., 1995).

## RESULTS OF TORSION SHEAR TESTS

Results of tests on Kiyohoro silty clay are shown in Figs. 3 through 6. Figure 3 shows the typical time history of the applied shear strain, together with the hysteresis loops for two different stages. In interpreting the results of the CL tests, a secant stiffness is defined as the slope of a line which connects the two peaks in a hysteresis loop. This is termed the equivalent shear modulus denoted as  $G_{eq}$  (see Figs. 3(b) and (c)). The relationship between  $G_{eq}$  and  $\gamma_{SA}$  is shown in Fig. 4, in which the variation between the secant shear modulus,  $G_{sec}$ , and  $\gamma$  for a ML test KY6 is also shown for comparison. Since shear strain was applied cyclically about  $\gamma=0$  in the CL tests, it is fair to compare these two relationships. In the CL tests,  $G_{eq}$  was

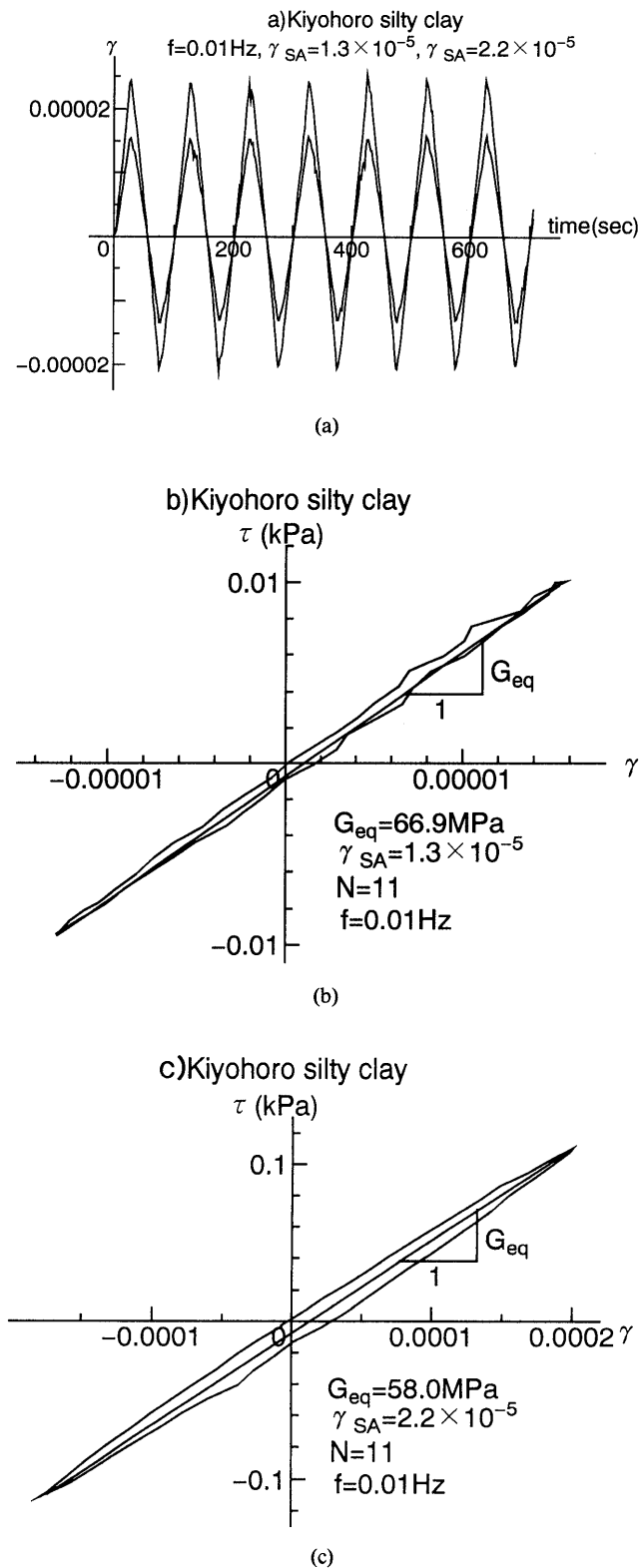


Fig. 3. Results of a test on Kiyohoro silty clay; (a) excitation of applied shear strain, and (b) and (c) hysteresis loops

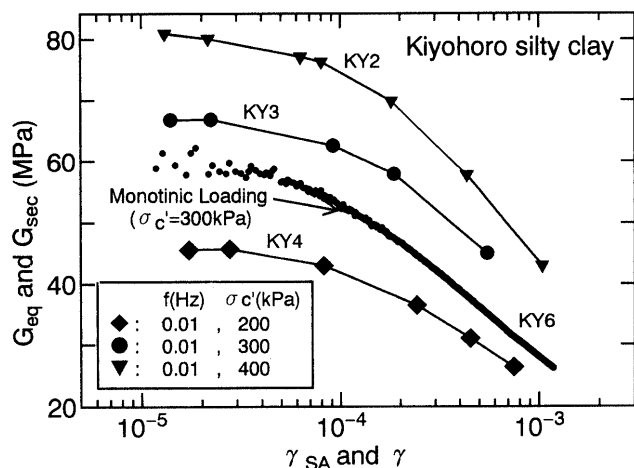


Fig. 4. Variation of shear moduli with shear strain in tests on reconstituted samples of Kiyohoro silty clay

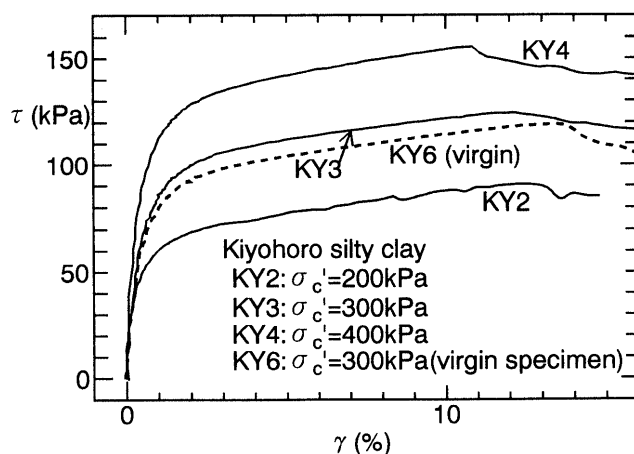


Fig. 6. Stress-strain relationship of reconstituted Kiyohoro silty clay during monotonic shear

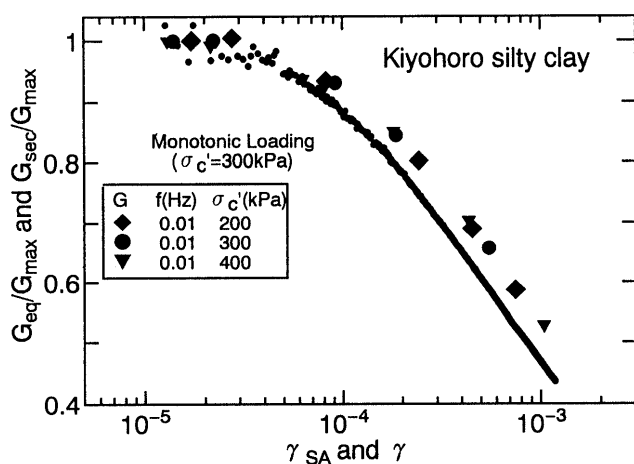


Fig. 5. Shear moduli normalized by  $G_{max}$  against shear strain for tests on reconstituted Kiyohoro silty clay

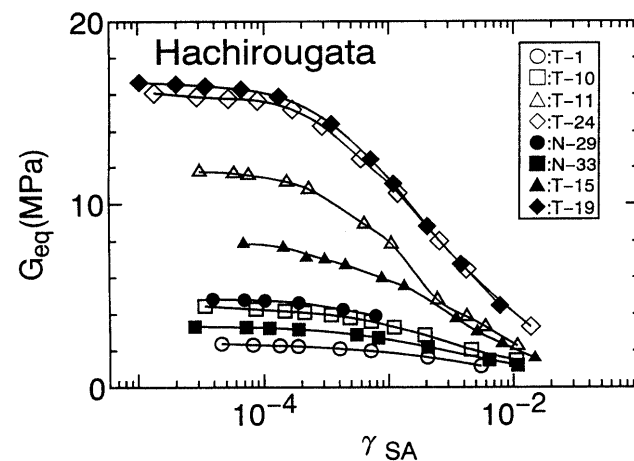


Fig. 7. Variation of shear moduli with shear strain in tests on undisturbed samples of Hachirougata clay

determined for each as the average of those for  $N$  from 2 to 20. It should be mentioned that variation of  $G_{eq}$  against  $N$  was not significant for all the stages. For each test, the pseudo-elastic shear modulus,  $G_{max}$ , was determined as the first data point with  $\gamma_{SA}$  less than 0.003% ( $3 \times 10^{-5}$ ). Similarly, in a ML test KY6, the  $G_{max}$  value was derived from a linear regression analysis for the  $\tau - \gamma$  relationship with  $\gamma$  less than 0.003% (Shibuya et al., 1995).

In Fig. 5, the shear moduli,  $G_{eq}$  and  $G_{sec}$ , normalized

by  $G_{max}$  are plotted against  $\gamma_{SA}$  and  $\gamma$ . It should be pointed out, that the decrease in shear moduli commenced at shear strains of about 0.003%, irrespective of the type of loading. The stiffness dropped down to approximately one-half that of  $G_{max}$  at shear strain of 0.1%. The normalized curves for the CL tests were remarkably similar for a range of  $\sigma'_c$  examined. The decrease in stiffness was slightly faster in the ML test than in the CL tests.

Figure 6 shows  $\tau - \gamma$  relationship for the subsequent stage of monotonic shear. In this figure, test KY6 implies the response of a virgin specimen which has previously not been subjected to cyclic loading. The undrained shear strength,  $C_u$ , refers to the maximum value of shear stress mobilized on the horizontal plane,  $\tau_{max}$ . The values of  $G_{max}$  and  $\tau_{max}$ , together with  $G_{sec}$  at  $\tau_{max}/2$ ,  $G_{50}$ , are shown in Table 2.

Figure 7 shows the relationship between  $G_{eq}$  and  $\gamma_{SA}$  for a total of eight Hachirougata samples obtained from different depths. Except for test N29 where some difficulty occurred in the testing, the stiffness was successfully measured over a wide scope of  $\gamma_{SA}$  between 0.003% and 1%. The normalized relationship is shown in Fig. 8, for

Table 2. Samples of reconstituted Kiyohoro silty clay

Test	$\sigma'_c$ (kPa)	$e_0$	$e_f$	$G_{max}$ (MPa)	$G_{50}$ (MPa)	$\tau_{max}$	$\frac{G_{max}}{\tau_{max}}$	$\frac{G_{50}}{\tau_{max}}$	$\frac{\tau_{max}}{\sigma'_c}$	$f$
KY2	200	0.731	0.729	45.5	11.8	91	500	130	0.45	0.01
KY3	300	0.709	0.708	66.8	13.9	124	539	112	0.42	0.01
KY4	400	0.683	0.680	80.9	20.3	156	519	130	0.39	0.01
KY6	300	0.705	0.705	59.4	14.3	119	499	120	0.40	—

N.B.:  $e_0$  and  $e_f$ : void ratio at the start and at the end of cyclic loading

which like Kiyohoro silty clay, the first data points with  $\gamma_{SA}$  less than 0.003% are taken as  $G_{max}$ . The influence of  $\sigma'_c$  shows a familiar trend that the decrease in  $G_{eq}$  is slightly faster for samples with higher  $\sigma'_c$ . It dropped to 70–80 percent and 25–40 percent of  $G_{max}$  at  $\gamma_{SA}$  equal to 0.1% and 1%, respectively. It should be mentioned, that the development of excess pore pressure during CL was virtually zero for the samples. And that the decrease in water content during the multi-stage cyclic loading was very small, at most 1.5% observed in specimen T1 (see Table 1).

**DISCUSSIONS**

*Compressibility of Normally Consolidated Clay -intact versus reconstituted samples*

A sedimentary clay is assumed to be uniform for its entire depth. Figure 9 shows simplified relationships between  $e$  and  $\sigma'_v$ . The straight line having a slope of  $C_c$  represents the relationship for natural sedimentation which has been formed over a geological period. According to Burland (1992), this is designated the sedimentary compression line (SCL). Similarly, the  $e - \log \sigma'_v$  relation for a reconstituted sample may also be approximated as a straight line, which has been designated the intrinsic compression line (ICL) with a compression index,  $(C_c^*)_{ICL}$ . When an undisturbed sample at point 'A' is consolidated in the laboratory to a stress level far beyond the in-situ  $\sigma'_v$ , the aspect of the compressibility may well be different from these. If the clay is highly structured, the state of the soil at the end of primary consolidation would approach asymptotically the ICL (Burland, 1992). If not, the laboratory compression line (LCL) may approach the line of 'instant compression' as pointed out by Bjerrm (1967). In this case, the compression index,  $(C_c^*)_{LCL}$ , results in a lower value than  $C_c$ . The difference in compressibility, which is depicted between  $C_c$  of the SCL and  $(C_c^*)_{LCL}$ , may be attributed to the "aging effect"; that is the original structure of the clay could be modified as  $\sigma'_v$  is increased beyond the in-situ value.

A comparison between SCL and LCL for Hachirougata clay is seen in Figs. 10 and 11. On the basis of the borehole data (see Fig. 1), the SCL is drawn as a result of a linear regression analysis (Fig. 10). Similarly, an LCL was obtained from test T2, in which  $\sigma'_c$  was increased in steps from in-situ mean effective stress of 25 kPa to 196 kPa (Fig. 11, see also Table 1). As discussed later, after completion of consolidation at each  $\sigma'_c$ , the sample was subjected to undrained cyclic shear using a fixed  $\gamma_{SA}$  equal to 0.002%. Swell index,  $C_s^*$ , was also examined for the subsequent unload-reload curve. In the case of this rather young clay, the compression index,  $(C_c^*)_{LCL}$ , was 1.92 which is smaller by a factor of about two compared to  $C_c$  associated with the SCL. The void ratio extrapolated at  $(\sigma'_v)_r=1$  kPa is also smaller for the LCL (i.e.,  $e_r^*=7.73$ ) than for the SCL (i.e.,  $e_r=10.87$ ). The inter-relationship between the SCL and LCL for Hachirougata clay basically exhibits the pattern of path A→a shown in Fig. 9.

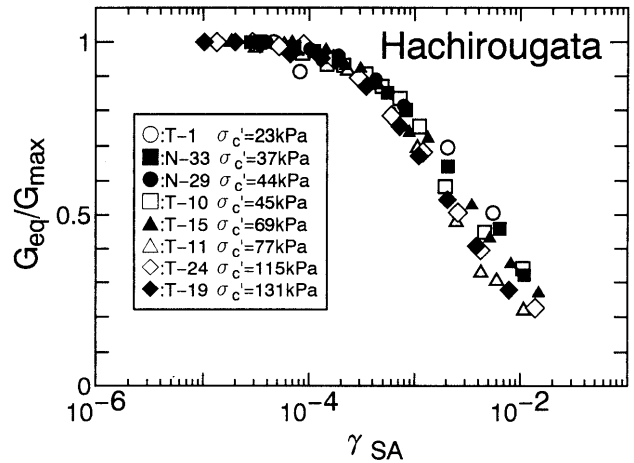


Fig. 8. Shear moduli normalized by  $G_{max}$  against shear strain in tests on undisturbed samples of Hachirougata clay

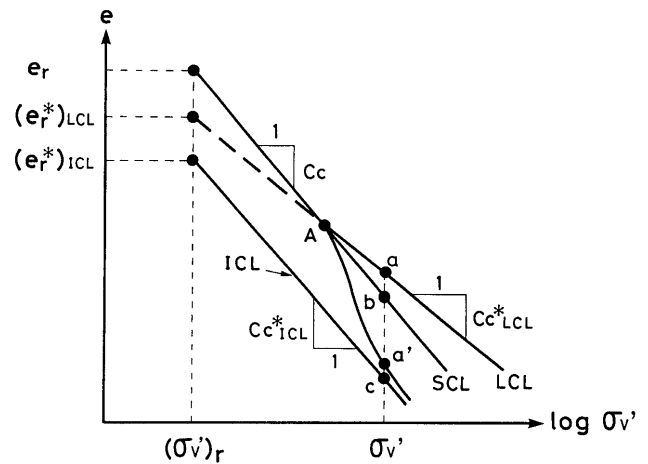


Fig. 9. Sedimentary compression line (SCL), intrinsic compression line (ICL) and laboratory compression line (LCL)

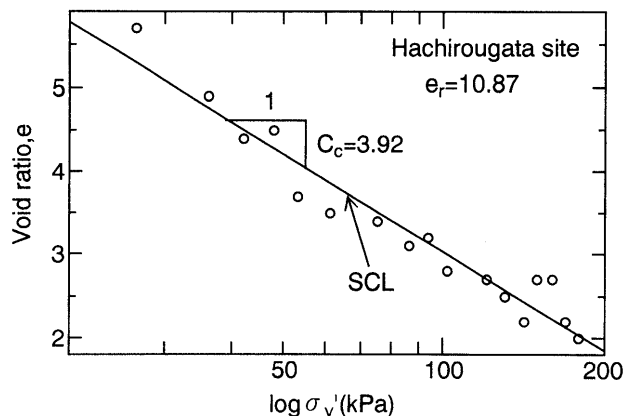


Fig. 10. Sedimentary compression line at Hachirougata site

It should be mentioned, that the  $e - \log \sigma'_c$  relationship for reconstituted Kiyohoro silty clay was also linear with the value of  $(C_c^*)_{ICL}$  equal to 0.32 as examined for  $\sigma'_c$  between 200 kPa and 500 kPa. The SCL for Kiyohoro silty

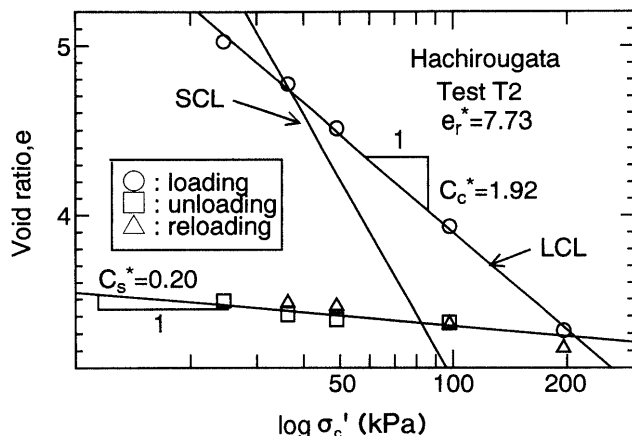


Fig. 11. A laboratory compression line of Hachirougata clay (test T2)

clay as well as the ICL for Hachirougata clay is not available so that the properties relevant to these are not discussed in this current study.

*Dependency of Shear Modulus on Stress and Strain Levels -interactions between in-situ and laboratory*

a) Formulation

In the following, an asterisk is used to denote properties of clay associated with either ICL or LCL, both of which are exclusively observed in the laboratory (see Fig. 9). As already shown in Figs. 10 and 11, the  $e - \log \sigma'_v$  relation for SCL and LCL as well as ICL can each be approximated as a straight line. These are given by:

$$e = e_r - C_c \log_{10} \{ \sigma'_v / (\sigma'_v)_r \} \quad \text{for SCL} \quad (3)$$

$$e^* = e_r^* - C_c^* \log_{10} \{ \sigma'_v / (\sigma'_v)_r \} \quad \text{for LCL} \quad (3')$$

where  $(\sigma'_v)_r$  and  $e_r$  (or  $e_r^*$ ) denotes the effective vertical stress at unity ( $=1$  kPa) and the void ratio at  $(\sigma'_v)_r$ , respectively (refer Fig. 9).

To the best of the authors' knowledge, the depth profile of shear modulus from seismic-type measurements is usually non-linear for a uniform clay deposit in the normally consolidated state (e.g., Oneda et al., 1984; Tanaka et al., 1994). Therefore, the shear modulus,  $G$ , may be conveniently expressed by the following equations:

$$G/G_r = \{ \sigma'_v / (\sigma'_v)_r \}^{m(\gamma)} \quad \text{for SCL} \quad (4)$$

$$G^*/G_r^* = \{ \sigma'_v / (\sigma'_v)_r \}^{m^*(\gamma)} \quad \text{for LCL} \quad (4')$$

in which  $G_r$  or  $G_r^*$  represents the shear modulus at  $(\sigma'_v)_r$ . The exponent,  $m(\gamma)$  or  $m^*(\gamma)$ , is considered to be a function of shear strain level (refer Iwasaki et al., 1978). It should be mentioned that the Cam clay model simulates a specific condition of  $m^*(\gamma)$  equal to unity, irrespective of shear strain level.

The relationship between  $G$  and  $e$  is thus given by;

$$G/G_r = \exp \{ m(\gamma)(e_r - e) / \lambda \} \quad (5)$$

$$G^*/G_r^* = \exp \{ m^*(\gamma)(e_r^* - e^*) / \lambda^* \} \quad (5')$$

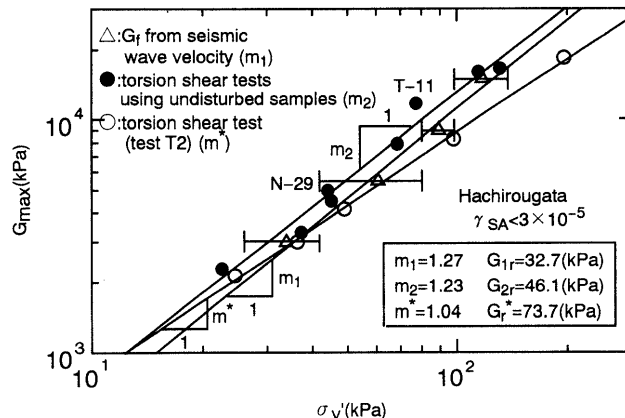


Fig. 12. Relationship between  $G_{max}$  and  $\sigma'_v$  for Hachirougata clay from in-situ seismic survey and cyclic torsion shear tests

in which  $(\lambda, \lambda^*)$  is equal to  $0.434 \times (C_c, C_c^*)$ . Combining Eqs. (4) and (5), the ratio of shear moduli,  $G^*/G$ , is expressed as follows:

$$G^*/G = (G_r^*/G_r) \cdot \{ \sigma'_v / (\sigma'_v)_r \}^{m^*(\gamma) - m(\gamma)} \quad (6)$$

$$G^*/G = (G_r^*/G_r) \exp \{ m^*(\gamma)(e_r^* - e^*) / \lambda^* - m(\gamma)(e_r - e) / \lambda \}. \quad (7)$$

Note that  $G^*/G$  is independent of  $\sigma'_v$  for the particular case when  $m^*(\gamma) = m(\gamma)$  (see Eq. (6)). The interrelationship between  $G^*$  and  $G$ , for example, those at points 'a' and 'b' in Fig. 9, may be governed by the coupled effects; the differences in the void ratio and the degree of aging under the current  $\sigma'_v$  between the original subsoil and the sample tested in the laboratory.

b) Examination based on results of in-situ and laboratory tests

Figure 12 shows the relationship between  $G_{max}$  and  $\sigma'_v$  for the Hachirougata clay. Three independent sets of data presented in this figure are: i)  $G_f$  from in-situ seismic shear wave velocity plotted against in-situ  $\sigma'_v$  (refer to Fig. 1), ii) the relationship between  $G_{max}$  and  $\sigma'_c$  for a total of eight cyclic torsion shear tests using undisturbed samples (refer to Fig. 7 and Table 1), and iii) the relation between  $G_{max}$  and  $\sigma'_c$  for test T2 (refer to Fig. 11). These relationships in this double-log plot may each be approximated as a straight line. The inclination of these solid lines (i.e.,  $m(\gamma)$  and  $m^*(\gamma)$ ), together with the shear modulus extrapolated at  $\sigma'_v = 1$  kPa,  $G_r$  and  $G_r^*$ , is shown in the inset. In the linear regression analysis for the second relation, no distinction is made for two groups of samples that could be distinguished in terms of  $\sigma'_c$  (i.e.,  $\sigma'_c$  equal to 1.0 and 2/3 of in-situ  $\sigma'_v$ ). In spite of some small scatter, good agreement is seen between the first and second relationships for both of which the SCL is the relevant consolidation curve. The third relationship associated with the LCL (see Fig. 11) indicates a value of  $m^*(\gamma)$  equal to unity, whereas the exponents for the others were more than unity (i.e.,  $m(\gamma) = 1.23$  and  $1.27$ ).

On the basis of the interrelationships amongst  $G_{max}$ ,  $\sigma'_v$  and  $e$  as shown in Figs. 10, 11 and 12, the ratio of  $G_{max}^*$

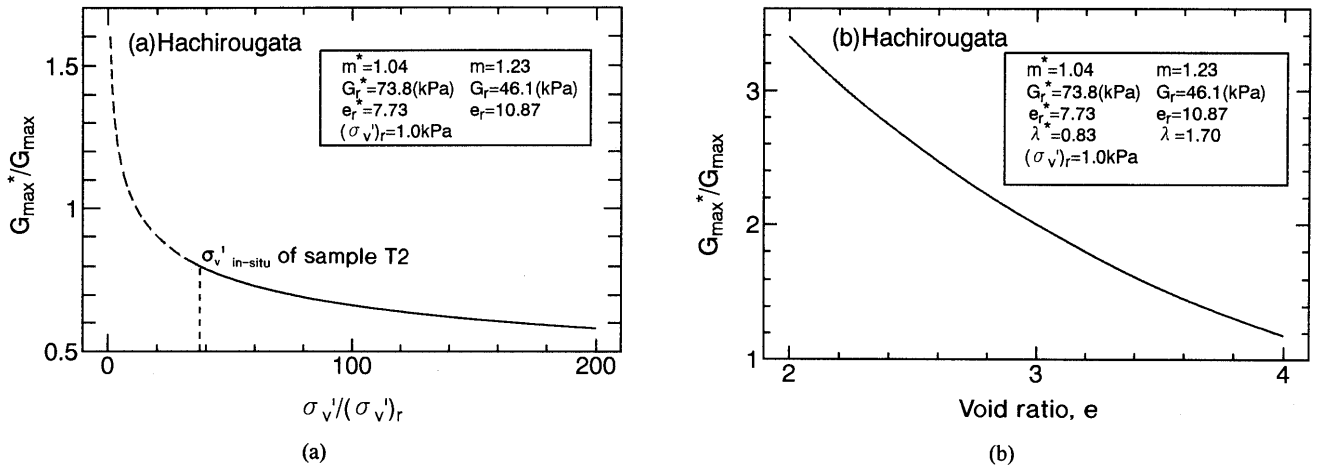


Fig. 13. Ratio of  $G_{max}$  on a laboratory compression line to  $G_{max}$  on the sedimentary compression: (a) in terms of  $\sigma'_v$ , and (b) in terms of void ratio

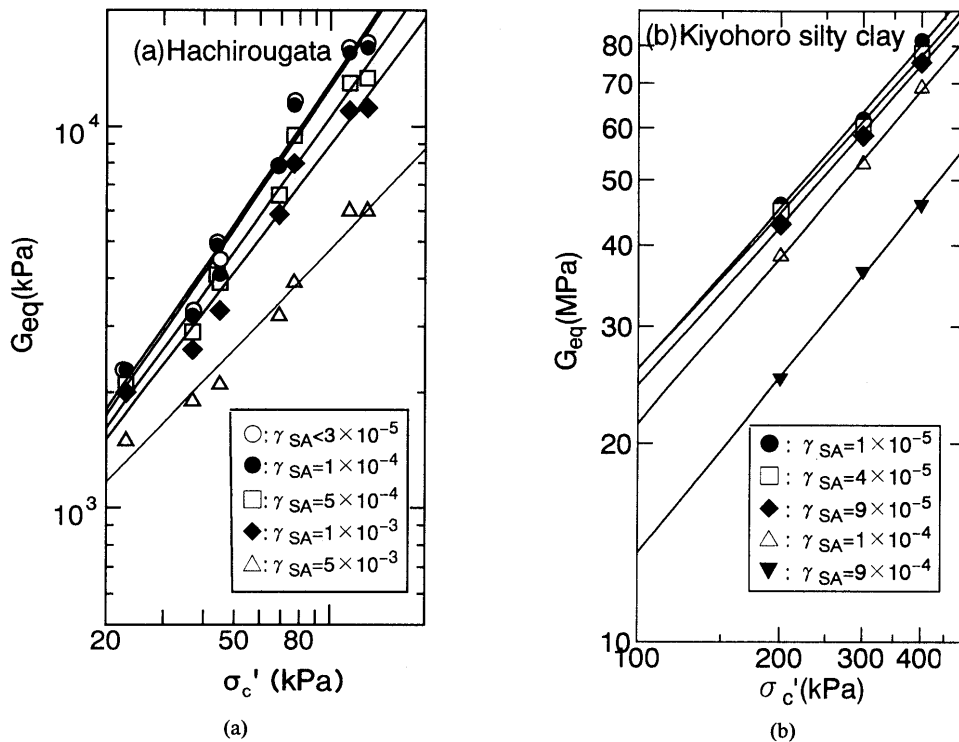


Fig. 14. Evaluation of exponents in Eqs. (4) and (4'); (a)  $m(\gamma)$  for undisturbed samples of Hachirougata clay, and (b)  $m^*(\gamma)$  for reconstituted Kiyohoro silty clay

on the LCL (i.e., relation iii) to  $G_{max}$  on the SCL (i.e., relation ii) was examined using Eqs. (6) and (7) (Fig. 13). The value is less than unity throughout as examined with respect to  $\sigma'_v$  (Fig. 13(a)). In addition, it gradually decreases from 0.78 to 0.66 for the range of  $\sigma'_v$  examined. This tendency originates from the fact that the value of  $m^*(\gamma) - m(\gamma)$  is negative (-0.19). The most important conclusion to be drawn is that the stress-level dependency of shear modulus in a natural clay deposit may never be correctly evaluated by using laboratory tests using samples that are re-consolidated beyond in-situ  $\sigma'_v$ . This is be-

cause the dependency of  $G_{max}$  on the stress level as well as the compressibility is different between SCL and LCL.

Results of analysis into  $m(\gamma)$  and  $m^*(\gamma)$  at larger strain levels are shown in Fig. 14. Note that for both the clays, the relation between  $G_{eq}$  and  $\sigma'_c$  for each  $\gamma_{SA}$  may be approximated as a straight line. The parameters obtained from Eqs. (4) and (4') are summarized in Table 3. In Fig. 15, the variations of  $m(\gamma)$  and  $m^*(\gamma)$  are shown for these three relationships. The following may be noted: i)  $m(\gamma)$  of Hachirougata intact clay remained constant at about 1.2 for  $\gamma_{SA}$  less than 0.01%, however, it gradually

decreased to 0.87 at  $\gamma_{SA}=0.5\%$ , ii)  $m^*(\gamma)$  of Kiyohoro silty clay remained more or less constant in a narrow range between 0.8 and 0.9 for  $\gamma_{SA}$  less than 0.1%, and iii)  $m^*(\gamma)$  of Hachirougata clay in test T2 was approximately unity at  $\gamma_{SA}$  equal to about 0.002%.

The variation of  $m(\gamma)$  may be unique for this particular type of clay deposit, in which,  $I_p$  decreases with depth (see Table 1) (Lo Presti, 1994). According to, for example, Dobry and Vucetic (1987), the decay of  $G_{eq}/G_{max}$  for a range of  $\gamma_{SA}$  larger than 0.1% becomes larger as the  $I_p$  of the clay decreases, which in turn results in an apparent decrease in  $m(\gamma)$ . The ‘‘aging effect’’ may be another key factor responsible for this. In a natural clay deposit, the sustained period of time under the current  $\sigma'_v$  is longer for the deeper samples with higher current  $\sigma'_v$ . As for the time effect on stiffness of clay, small strain shear modulus increased in proportion to the logarithm of the consolidation time (Anderson and Woods, 1976). Thus, it may be assumed that the increase in sustained period with depth brought about the value of  $m(\gamma)$  in excess of unity as observed for  $\gamma_{SA}$  less than 0.01%. The ‘‘aging effect’’ would disappear as the shear strain is large enough to cause rearrangements of the original clay structure which had been formed over the geological period. It is interesting to note that this particular strain level of 0.01% coincides with the threshold strain at which a build-up of volumetric strain, or excess pore pressure if undrained, commences as clay samples are subjected to cyclic loading (Dobry et al., 1982; Jardine, 1992; Shibuya et al., 1995). Consequently, the value of  $m(\gamma)$  at intermediate strains approached the value of about 0.9, which was close to  $m^*(\gamma)$  for the very young reconstituted clay.

c) Rigidity Index

The ratio of shear modulus to the undrained shear strength,  $G/C_u$ , is usually termed the rigidity index, which is frequently used as a design parameter in numerical analysis (Shibata and Soelarno, 1978). However, examination into  $G/C_u$  of clay is often made using  $G_{50}$  associated with intermediate strains in the order of 1% (e.g., Houlsby and Wroth, 1991).

In general, the undrained shear strength ratio,  $\alpha$  or  $\alpha^*$ , for undisturbed or reconstituted clays, is given by;

$$C_{ur}/(\sigma'_v)_r = C_u/\sigma'_v = \alpha \tag{8}$$

$$C_{ur}^*/(\sigma'_v)_r = C_u^*/\sigma'_v = \alpha^* \tag{8'}$$

Table 3. Results of linear regression analysis (refer Fig. 14)

Hachirougata clay					
$\gamma_{SA}$	$3 \times 10^{-5}$	$1 \times 10^{-4}$	$5 \times 10^{-4}$	$1 \times 10^{-3}$	$5 \times 10^{-3}$
$m(\gamma)$	1.23	1.23	1.17	1.10	0.87
$G_r$ (kPa)	46	44	49	55	86
Kiyohoro silty clay					
$\gamma_{SA}$	$1 \times 10^{-5}$	$4 \times 10^{-5}$	$9 \times 10^{-5}$	$1 \times 10^{-4}$	$9 \times 10^{-4}$
$m^*(\gamma)$	0.82	0.79	0.81	0.84	0.88
$G_r^*$ (kPa)	593	681	589	451	234

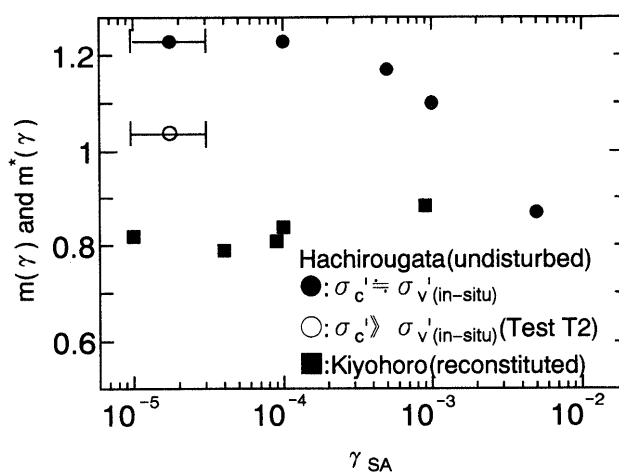


Fig. 15. Variations of  $m(\gamma)$  and  $m^*(\gamma)$  with single amplitude cyclic shear strain

in which  $C_{ur}$  (or  $C_{ur}^*$ ) refers to the value at  $(\sigma'_v)_r$ . It is believed that the values of  $\alpha$  and  $\alpha^*$  are each constant for a given clay in the normally consolidated state. The above equation when coupled with Eq. (4) gives the following;

$$G/C_u = (G_r/\alpha) \cdot \sigma'_v \{m(\gamma)-1\} \cdot (\sigma'_v)_r \{m(\gamma)-1\} \tag{9}$$

$$G^*/C_u^* = (G_r^*/\alpha^*) \cdot \sigma'_v \{m^*(\gamma)-1\} \cdot (\sigma'_v)_r \{m^*(\gamma)-1\} \tag{9'}$$

The condition of  $m(\gamma)$  and  $m^*(\gamma)$  equal to unity implies that the rigidity index is constant for  $\sigma'_v$ . The index is dependent of  $\sigma'_v$  such that it increases and decreases in value with depth as the exponent is larger than and smaller than unity, respectively.

For undisturbed samples of Hachirougata clay,  $\alpha$  equal to 0.33 is obtained from direct shear box tests (Fig. 16). Similarly, the value of  $\alpha^*$  was 0.40 for the virgin specimen of Kiyohoro silty clay, that is test KY6 (see Table 2). The variation of rigidity index with  $\sigma'_v$  is shown in Fig. 17. For both of these clays, the relationship is derived from Eqs. (9) or (9') using the measured parameters of  $(\alpha, m(\gamma), G_r)$  or  $(\alpha^*, m^*(\gamma), G_r^*)$  (see Table 3). It is obvious that the rigidity index strongly depends on the shear strain level even at small strains less than 0.1%. The rigidity index of Hachirougata clay showed a substantial increase with depth for  $\gamma_{SA}$  less than 0.1%, and vice versa for  $\gamma_{SA}$  larger than 0.1%. Rigidity index for reconstituted Kiyohoro silty clay decreased slightly as  $\sigma'_v$  increased. The trends are in agreement with the variations of  $m(\gamma)$  and  $m^*(\gamma)$ , which are shown in Fig. 15. It should also be pointed out that for Kiyohoro silty clay, the values of  $G_{50}/C_u$  are much smaller than those at small strains (see Table 2). These results strongly suggest that the use of  $G_{50}$  is inappropriate for most of deformation problems, and that the shear strain level as well as in-situ stress level under working conditions should be properly evaluated when applying the rigidity index to actual design problems.

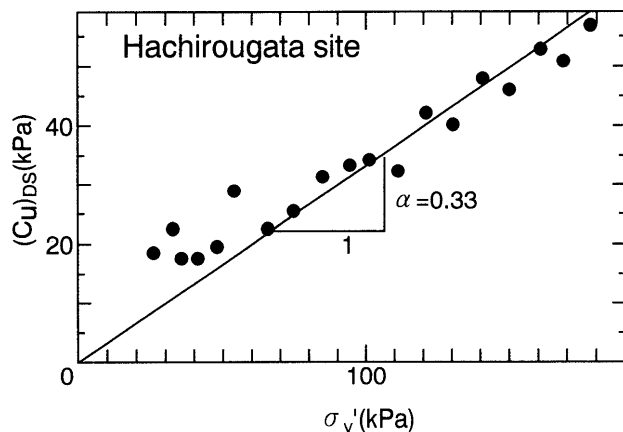


Fig. 16. Undrained shear strength of Hachirougata clay from direct shear box tests (Tang et al., 1993)

## CONCLUSIONS

Properties of small strain shear modulus of clay focused on the interactions between in-situ and laboratory are summarized as follows:

1) In a sedimentary clay such as at the Hachirougata site, the void ratio decreases linearly with the logarithm of the effective overburden pressure,  $\sigma_v'$ . The slope of the sedimentary compression line (SCL) was about twice that of the laboratory compression line (LCL) of an undisturbed sample which was consolidated to a stress level far beyond in-situ  $\sigma_v'$ . In some other marine clays in Japan, the void ratio is not directly related to in-situ  $\sigma_v'$  (Shibuya, 1995).

2) The depth profile of shear modulus from an in-situ seismic survey was practically identical to the stress-level dependency of shear modulus at extremely small shear strain,  $\gamma$ , of about 0.002%, which was obtained from laboratory cyclic loading tests using undisturbed samples.

3) The shear modulus of the normally consolidated clay can be quantified in Eqs. (4) and (4'). The power,  $m(\gamma)$ , of a natural clay sedimentation at the Hachirougata site was about 1.3 for  $\gamma$  between 0.001% and 0.01%, and gradually decreased to about 0.9 at  $\gamma$  equal to 0.5%. The power,  $m^*(\gamma)$ , for reconstituted Kiyohoro silty clay was rather independent of  $\gamma$ , and remained in a narrow range between 0.8 and 0.9 as examined for  $\gamma$  between 0.001% and 0.1%.

4) The stress-level dependency of the shear modulus in a natural clay deposit may never be correctly evaluated by laboratory tests using undisturbed samples that are re-consolidated beyond in-situ  $\sigma_v'$ . This is attributed mainly to the differences in compressibility and in "aging effect" between in-situ and laboratory conditions.

5) The stress-level dependency of the rigidity index can be quantified by Eqs. (9) and (9'). For the Hachirougata and reconstituted Kiyohoro silty clay, the ratio of secant shear modulus to undrained shear strength was roughly 300 ~ 500 and 500 ~ 600 at shear strain equal to 0.001%, respectively, and for each soil reduced to one half of it at

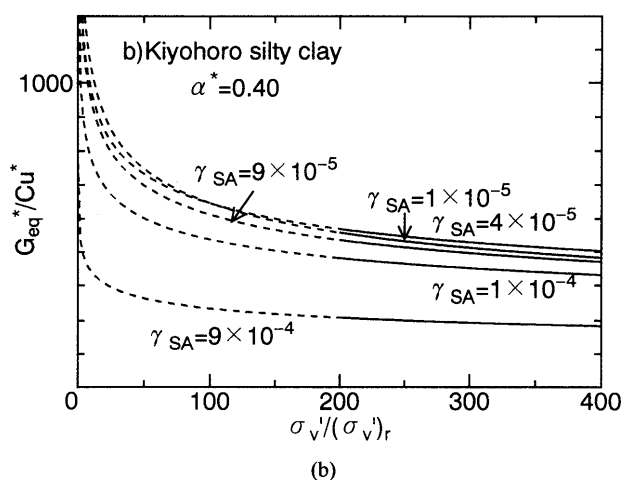
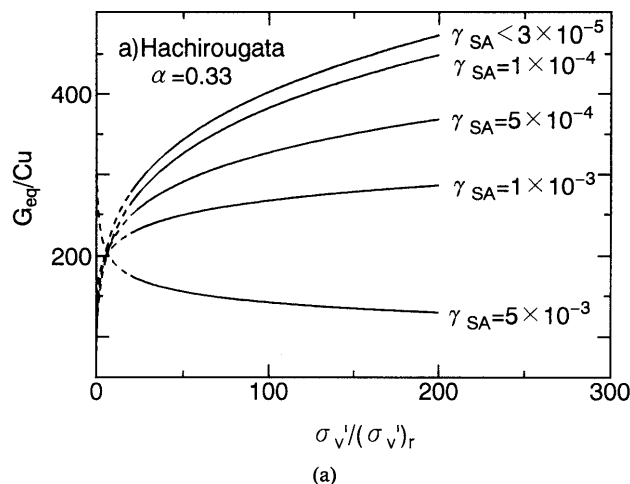


Fig. 17. Variation of rigidity index with stress and strain levels; (a) Hachirougata clay, and (b) reconstituted Kiyohoro silty clay

shear strain of 0.1%. The dependency of rigidity index on stress level is principally governed by the value of the exponent,  $m(\gamma)$  or  $m^*(\gamma)$  (see Eqs. (4) and (4')).

When predicting or analyzing ground deformation, it is considered important to use the rigidity index in order to match the in-situ strain level as well as the stress level under working conditions.

## ACKNOWLEDGEMENTS

The authors are indebted to Dr. H. Tanaka, Port and Harbour Research Institute, and Dr. H. Hanzawa, Toa Corporation, for in-situ test data provided from the Hachirougata site. Messrs T. Hosono and M. Nakajima, Dia Consultant Co. Ltd., F. Fukuda, Y. Kudo, T. Degoshi and H. Mino, our colleagues and students, are also acknowledged for their help in performing laboratory tests and in preparing the manuscript. Part of the research was supported by TEPCO Research Foundation.

## REFERENCES

- 1) Anderson, D. G. and Woods, R. G. (1976): "Time-dependent in-

- crease in shear modulus of clay," Jour. of Geotech. Engr. Div., Proc. of ASCE, Vol. 102, No. GT5, pp. 525-537.
- 2) Atkinson, J. H. (1993): "A note on modelling small strain stiffness in Cam clay," Predictive Soil Mechanics, Thomas Telford, London, pp. 111-120.
  - 3) Bjerrum, L. (1967): "Engineering geology of Norwegian normally-consolidated marine clays as related to settlements of buildings," Seventh Rankine Lecture, Géotechnique, Vol. 17, No. 2, p. 81-118.
  - 4) Burland, J. B. and Symes, M. J. (1982): "A simple axial displacement gauge for use in triaxial apparatus," Géotechnique, Vol. 32, No. 1, pp. 62-65.
  - 5) Burland, J. B. (1989): Ninth L. Bjerrum Memorial Lecture "Small is beautiful—the stiffness of soils at small strains," Canadian Geotech. Jour., Vol. 26, pp. 499-516.
  - 6) Burland, J. B. (1992): "On the compressibility and shear strength of natural clays," 30th Rankine Lecture, Géotechnique, Vol. 40, No. 3, pp. 329-378.
  - 7) Dobry, R. L., Ladd, R. S., Yokel, F. Y., Chung, R. M. and Powell, D. (1982): "Prediction of pore pressure build up and liquefaction of sands during earthquakes by the cyclic strain method," National Bureau of Standards, Building and Technology Science Series 138, US Department of Commerce.
  - 8) Dobry, R. L. and Vucetic, M. (1987): "Dynamic properties and seismic response of soft clay deposits," Proc. of Inter. Sympo. on Geotech. Engr. of Soft Soils, Mexico City, Vol. 2, pp. 51-87.
  - 9) Duncan, J. M. and Chang, C. Y. (1970): "Nonlinear analysis of stress and strain in soils," Jour. of SMF Div., ASCE, Vol. 96, No. SM5, pp. 1629-1653.
  - 10) Goto, S., Tatsuoka, F., Shibuya, S., Kim, Y.-S. and Sato, T. (1991): "A simple gauge for local small strain measurements in the laboratory," Soils and Foundations, Vol. 31, No. 1, pp. 169-180.
  - 11) Hardin, B. O. and Drnevich, V. P. (1972): "Shear modulus and damping in soils: Measurement and parameter effects," Jour. of the SMF Div., Proc. ASCE, Vol. 98, No. SM6, pp. 603-624.
  - 12) Hight, D. W., Gens, A. and Symes, M. J. (1983): "The development of a new hollow cylinder apparatus for investigating the effects of principal stress rotation in soils," Géotechnique, Vol. 33, No. 4, pp. 355-383.
  - 13) Houlsby, G. T. and Wroth, C. P. (1991): "The variation of shear modulus of a clay with pressure and overconsolidation ratio," Soils and Foundations, Vol. 31, No. 3, pp. 138-143.
  - 14) Iwasaki, T., Tatsuoka, F. and Takagi, Y. (1978): "Shear moduli of sands under cyclic torsional shear loading," Soils and Foundations, Vol. 18, No. 1, pp. 39-56.
  - 15) Jardine, R. J., Potts, D. M., Fourie, A. B. and Burland, J. B. (1986): "Studies of non-linear stress-strain characteristics in soil-structure interaction," Géotechnique, Vol. 36, No. 3, pp. 377-396.
  - 16) Jardine, R. J. (1992): "Some observations on the kinematic nature of soil stiffness," Soils and Foundations, Vol. 32, No. 2, pp. 111-124.
  - 17) Kondner, R. B. (1963): "Hyperbolic stress-strain response: cohesive soils," Jour. of SMF Div., Proc. ASCE, Vol. 89, No. SM1, pp. 115-143.
  - 18) Lo Presti, D. C. F. (1994): Personal communications.
  - 19) Oneda, H., Umehara, Y., Higuchi, Y. and Irisawa, K. (1984): "Engineering properties of marine clay in Osaka Bay (Part 4); Dynamic stress-strain and strength properties," Technical note of the Port and Harbour Research Institute, Ministry of Transportation, Japan, No. 498, pp. 115-136 (in Japanese).
  - 20) Shibata, T. and Soelarno, D. S. (1978): "Stress-strain characteristics of clays under cyclic loading," Jour. of JSCE, No. 276, pp. 101-110 (in Japanese).
  - 21) Shibuya, S., Tatsuoka, F., Teachavorasinskun, S., Kong, X. J., Abe, F. Kim Y.-S. and Park, C.-S. (1992): "Elastic deformation properties of geomaterials," Soils and Foundations, Vol. 32, No. 3, pp. 26-46.
  - 22) Shibuya, S., Mitachi, T., Fukuda, F. and Degoshi, T. (1995): "Strain rate effects on shear modulus and damping of normally consolidated clay," Geotechnical Testing Jour., Vol. 18, No. 1 (in press).
  - 23) Shibuya, S. (1995): "Characterization of small strain shear modulus of Tokyo Bay clay," Proc. of 11th European Regional Conf. on SMFE, Copenhagen (in press).
  - 24) Tanaka, H., Tanaka, M., Iguchi, H. and Nishida, K. (1994): "Shear modulus of soft clay measured by various kinds of tests," Pre-failure Deformation of Geomaterials (S. Shibuya, T. Mitachi and S. Miura eds), Balkema, Vol. 1, pp. 235-240.
  - 25) Tang, Y. X., Hanzawa, H. and Tanaka, H. (1993): "Quality and shear strength of undisturbed clay sample obtained by various types of samplers," Proc. Int. Conf. on Soft Soil Eng., Guangzhou, China, pp. 809-815.
  - 26) Tatsuoka, F. and Shibuya, S. (1992): "Deformation characteristics of soils and rocks from field and laboratory tests," Keynote Lecture, Proc. of 9th Asian Regional Conf. on SMFE, Vol. 2, pp. 101-170.
  - 27) Teachavorasinskun, S., Shibuya, S. and Tatsuoka, F. (1991): "Stiffness of sands in monotonic and cyclic loading in simple shear," Proc. ASCE Geotech. Eng. Conf., Boulder, Geotech. Special Publication No. 27, Vol. 1, pp. 863-878.

## NOTATION

- $\sigma'_c$ : isotropic consolidation pressure applied to laboratory specimens  
 $\sigma'_y$ : yield stress from standard oedometer test  
 $\sigma'_v$ : in-situ overburden pressure  
 SCL: sedimentary compression line defined for the relationship between void ratio,  $e$ , and effective overburden pressure,  $\sigma'_v$ , of natural clay deposit  
 ICL: intrinsic compression line defined for the relationship between void ratio,  $e$ , and consolidation pressure,  $\sigma'_c$ , of reconstituted clay samples  
 LCL: laboratory compression line defined for the  $e - \sigma'_c$  relationship of natural clay samples obtained using  $\sigma'_c$  in excess of in-situ  $\sigma'_v$ .  
 $C_c$ : compression index  
 $C_u$ : undrained shear strength  
 $\rho_t$ : total mass of soil  
 $V_s$ : in-situ shear wave velocity  
 $\tau_{max}$ : maximum shear stress mobilized in monotonic loading test  
 $\gamma_{SA}$ : single amplitude cyclic shear strain in cyclic loading test  
 $\gamma$ : shear strain in monotonic loading test  
 $G_{max}$ : maximum shear modulus associated with shear strains less than 0.002%  
 $G_f$ : shear modulus from in-situ seismic survey ( $=\rho_t V_s^2$ )  
 $G_{eq}$ : equivalent shear modulus in cyclic loading test  
 $G_{sec}$ : secant shear modulus in monotonic loading test  
 $G_{50}$ : secant shear modulus at a half of  $\tau_{max}$   
 $\alpha$ :  $C_u/\sigma'_c$  or  $C_u/\sigma'_v$   
 $m(\gamma)$ : exponent  
 A superscript "\*" denotes soil properties associated with ICL and/or LCL  
 A subscript "r" means properties defined at the reference stress of 1.0 kPa